The gauche-trans Energy Difference of n-Butane from a Doppler Limited Investigation of the 740 cm^{-1} CH_2-Rocking Region

G. Gassler and W. Hüttner

Abteilung Chemische Physik, Universität Ulm, Ulm, West Germany

Z. Naturforsch. **45a**, 113–125 (1990); received June 20, 1989

Tunable diode laser spectra of n-butane gas were recorded in the 740 cm^{-1} CH_2-rocking region using path lengths of typically 300 m, pressures below 1 mbar and temperatures between 170 and 300 K. The spectra are complicated by the overlap of the two trans and gauche rotameric fundamentals, and by a strong absorption background probably caused by the addition of hot-band transitions involving excitation of one or more quanta of the torsion vibrations around the central C–C bond. Analysis was aided by Fourier transform recordings in medium and high resolution and lead to the assignment of rovibrational features close to the band centers at ν_0(trans) = (733.5797 ± 0.0015) cm^{-1} and ν_0(gauche) = (747.5116 ± 0.0018) cm^{-1} of the trans and gauche rotamers, respectively, and to medium accurate spectroscopic parameters. A statistical evaluation of the temperature dependence of the relative absorption intensities of near-by trans and gauche transitions resulted in the trans-gauche rotameric energy difference of ΔH = (246 ± 18) cm^{-1} or (2.94 ± 0.21) kJ mol^{-1}. This value is lower than those from previous determinations but still indicates an interesting decrease of the gauche-trans energy difference in going from gas to the liquid state.

Key words: n-Butane, Rotamers, Diode laser spectra, FTIR spectra, trans-gauche Energy difference.

1. Introduction

n-Butane, $CH_3CH_2-CH_2CH_3$, is the first member of the alkane series showing rotational isomerism. It exists in two stable forms, trans and gauche, where the former, as first established by Szasz, Sheppard, and Rank [1], is lower in energy. An accurate knowledge of the gauche-trans energy difference ΔH and of the dihedral potential function around the central carbon-carbon bond would be of great value for understanding the dynamics of chain perturbations in polyethylene, a model system for the investigation of polymer melts and solutions.

The standard procedure for determining ΔH, the difference of the gauche and trans zero-point vibrational energies, is based on the temperature dependence of the relative intensities of vibrational transitions of the different rotameric forms. In this way, Verma, Murphy, and Bernstein have determined ΔH from the Raman effect of n-butane in the gaseous state [2]. Other methods involved gas-phase electron diffraction [4] and fitting on experimental heat capacity and entropy data [3]. Compton, Montero, and Murphy have fitted the torsional fundamentals and torsional hot-band transitions of the n-butane system to a set of dihedral-potential expansion coefficients, and then obtained ΔH from the resulting function [5]. The authors claim consistence of their result with thermodynamic data [5]. However, it seems difficult to assign unequivocally the weak and sometimes overlapping vibrational bands in the region below 250 cm^{-1}, as can be seen from a recent discussion by Stidham and Durig [6]. These authors reassigned partly the spectra of Compton et al. [5] and arrived, in combining them with their own far-infrared data, at a potential curve which showed a markedly lower trans-cis barrier. In their analysis, Stidham and Durig did not determine ΔH but included it, as a low-weighted quasi-experimental information, in the set of torsional frequencies. The ΔH value was taken from the most recent ab-initio investigation of the n-butane system carried out by Raghavachari [7]. Noteworthy, the ab-initio potential function itself [7] culminates in a still higher trans-cis barrier as compared with the result of Compton et al. [5].

So far, only gas-phase investigations have been discussed. The differing numerical results of ΔH obtained in the cited publications have been collected in Table 1. Earlier experimental and theoretical work is reviewed, for example, in [7]. As one can see, there is a considerable scatter in the values. The most recent

Reprint requests to Prof. Dr. W. Hüttner, Universität Ulm, Abteilung Chemische Physik, D-7900 Ulm, FRG.

0932-0784 / 90 / 0200-0113 $ 01.30/0. – Please order a reprint rather than making your own copy.

Dieses Werk wurde im Jahr 2013 vom Verlag Zeitschrift für Naturforschung in Zusammenarbeit mit der Max-Planck-Gesellschaft zur Förderung der Wissenschaften e.V. digitalisiert und unter folgender Lizenz veröffentlicht: Creative Commons Namensnennung-Keine Bearbeitung 3.0 Deutschland Lizenz.

This work has been digitalized and published in 2013 by Verlag Zeitschrift für Naturforschung in cooperation with the Max Planck Society for the Advancement of Science under a Creative Commons Attribution-NoDerivs 3.0 Germany License.

Zum 01.01.2015 ist eine Anpassung der Lizenzbedingungen (Entfall der Creative Commons Lizenzbedingung „Keine Bearbeitung") beabsichtigt, um eine Nachnutzung auch im Rahmen zukünftiger wissenschaftlicher Nutzungsformen zu ermöglichen.

On 01.01.2015 it is planned to change the License Conditions (the removal of the Creative Commons License condition "no derivative works"). This is to allow reuse in the area of future scientific usage.

Table 1. Gauche-trans energy difference of n-butane from different methods of determination [a].

Method	ΔH		Ref.
	kJ mol^{-1}	cm^{-1}	
Gas:			
Raman intensities	4.04 (23)	338 (19)	[2]
Thermodynamic data	3.18	266	[3]
Electron diffraction [b]	3.14 (103)	263 (86)	[4]
Raman torsional analysis	3.72 (12)	311 (10)	[5]
ab-initio calculation [c]	2.72 (30)	227 (35)	[7]
Rovibrational intensities, this work [b]	2.94 (21)	246 (18)	
Liquid:			
Raman intensities	2.33 (5)	195 (4)	[8]

[a] Errors are given in parentheses in units of the least significant figure.
[b] Error based on three standard deviations.
[c] Error estimated from variations with different basis sets.

results of Kint, Scherer, and Snyder [8] obtained in the liquid phase from the temperature dependence of Raman band intensities are also included in the table. The liquid-phase Raman intensity method is the most direct approach, and is expected to be less sensitive against systematic errors than the experiments employed in [2]–[5]. It arises, therefore, the question whether the trend towards higher n-butane gauche-trans energy differences in the gaseous (free molecule) phase is real or not. Pratt, Hsu, and Chandler [9], using statistical mechanics, predicted an effective increase of 0.7 kJ mol^{-1} on grounds of molecular packing effects in the liquid, but this was not confirmed to this extent later on by Jorgensen [10] in computer simulations.

The gas-phase Raman method [2], though in closest analogy to that used in [8], suffers from the overlap of rotationally unresolved bands. The large value of 4 kJ mol^{-1} [2] is, therefore, rather doubtful. With present Doppler limited infrared techniques one can resolve single rovibrational transitions, hence it seems natural trying to determine ΔH by measuring the temperature variation of the intensities of single trans and gauche rotational fine structure components in a vibrational spectrum. In our present approach, we follow this line and mainly employ diode laser (DL) spectroscopy at low n-butane sample pressures and different temperatures. The investigation is aided by high-resolution Fourier transform infrared (FTIR) spectroscopy at room temperature.

For experimental reasons, it is essential to monitor the relative intensities of closely spaced trans and gauche rovibrational transitions. We have, therefore, selected the overlapping in-phase CH_2-rocking fundamentals centered near 733 cm^{-1} (trans) and near 748 cm^{-1} (gauche) for our investigation. It will be shown below that, for evaluating the intensity data, knowledge of the ground-state energies of the selected transitions is required, relative to their corresponding trans and gauche zero-point levels. We have, therefore, attempted to gain some insight in the rotational structure of the quoted n-butane fundamentals. As will be seen in the next section, the Doppler limited rovibrational CH_2-rocking spectrum of n-butane emerges weakly from an unusually strong, continuous absorption background which aggravated the analysis and asked for help from other sources. In a preceding DL spectroscopic study we have assigned the fine structure of the analogue CH_2-rocking fundamental of the propane molecule [11], the third member of the alkane series, which does not show isomerism around a carbon-carbon bond. This experience turned out to be helpful especially for analysing the trans n-butane CH_2-rocking mode. In order to facilitate assignments in the corresponding gauche fundamental we have determined the ground state spectroscopic constants of the n-butane rotamer using mm wave spectroscopy [12]. In this way it was possible to unravel parts of the rather dense rovibrational spectrum and to determine medium accurate spectral parameters for the ground and excited vibrational state of trans butane and for the excited rovibrational state of the gauche conformer.

2. Experimental

The basic DL spectrometer set-up and recent alterations have been described in [13] and [11], respectively. Butane gas was found much less absorptive in the 740 cm^{-1} region than the previously investigated propane [11].

In order to avoid pressure broadening, the spectra were recorded at pressures below 10^{-3} bar, using a newly constructed White type cell of almost 4 m length to provide effective path lengths of more than 500 m. The three mirrors [14] were cut from a Zerodur glass sphere of 3.7 m radius and of 0.15 m lateral diameter, and then silver coated. The diameter is large enough to prevent interference of neighbouring reflections, hence perturbing fringes are not seen. In addition, to induce such fringes in the present cell a coher-

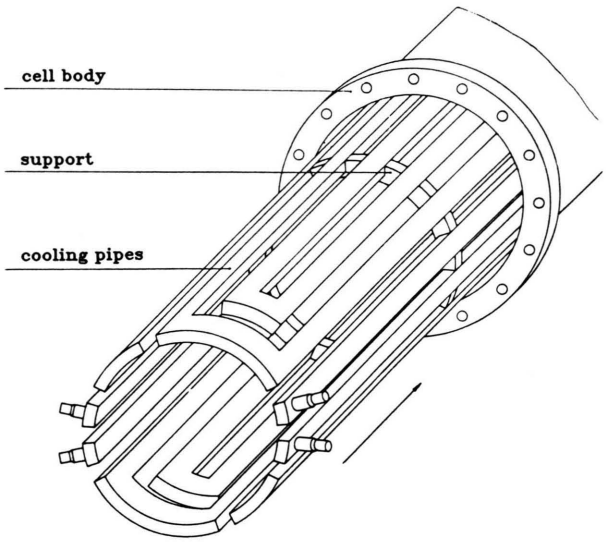

ence length of more than 16 m is required, which might be too long for most laser diodes. The imaging properties of the set-up is excellent because of the small off-axis angles necessary for feeding in and out the laser beam. Two systems of cooling pipes of altogether 76 m length were installed in the cell corpus in the manner shown in Figure 1. There is only week thermal contact between the pipes and the corpus, and the cell is well insulated from the outside, in a block of styrene.

Two TDL spectra of n-butane gas, obtained with this cell assembly in the frequency range between 758.1 cm^{-1} and 759.0 cm^{-1} at temperatures 25 °C

Fig. 1. Cooling pipes for the 4 m White-type cell, to be installed within the cell body for immediate contact with the probe gas.

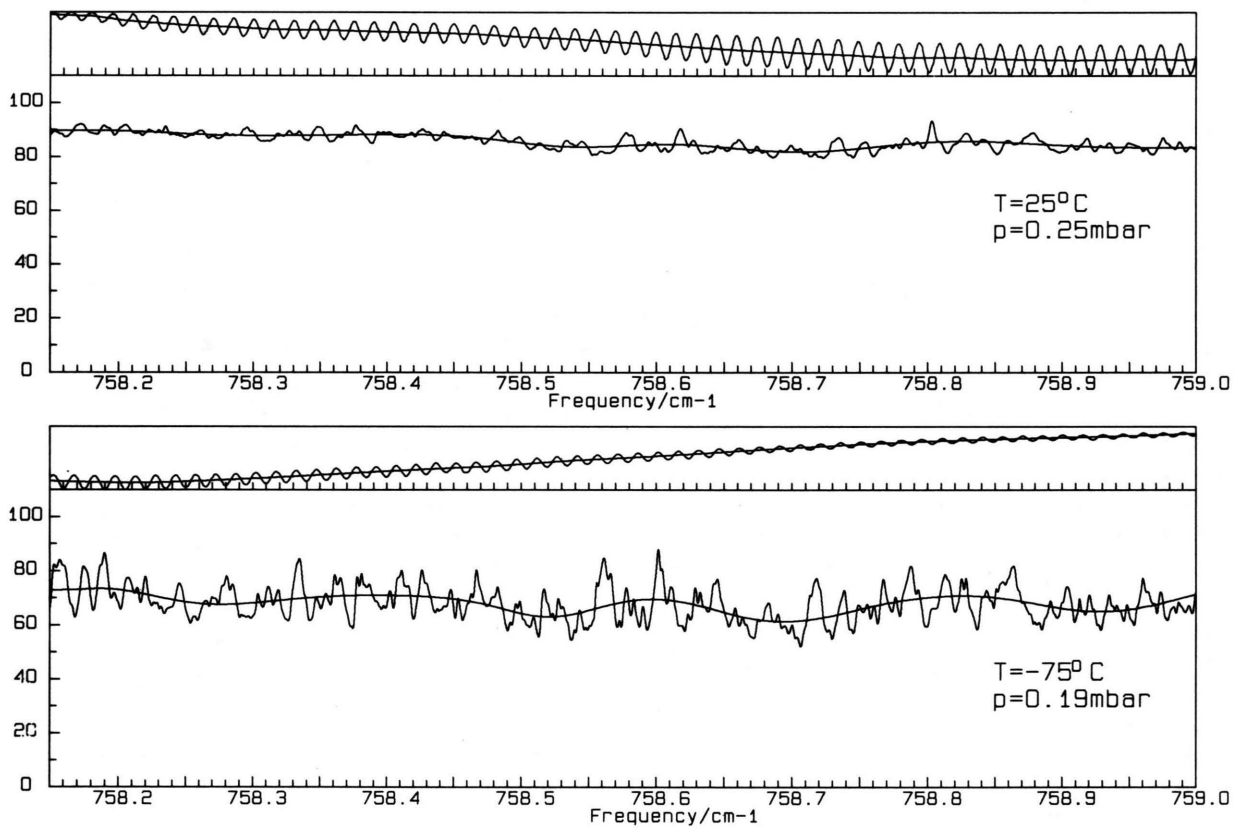

Fig. 2. TDL spectra of n-butane gas at two temperatures and 300 m path length in the White cell. The linear frequency scale was generatd by computer. The horizontal curves serve as intensity thresholds for automatic peak finding. The strong background is typical for the trans-gauche CH_2-rocking region (the ordinate scale means per cent absorption, fringe patterns are given on top of each spectrum).

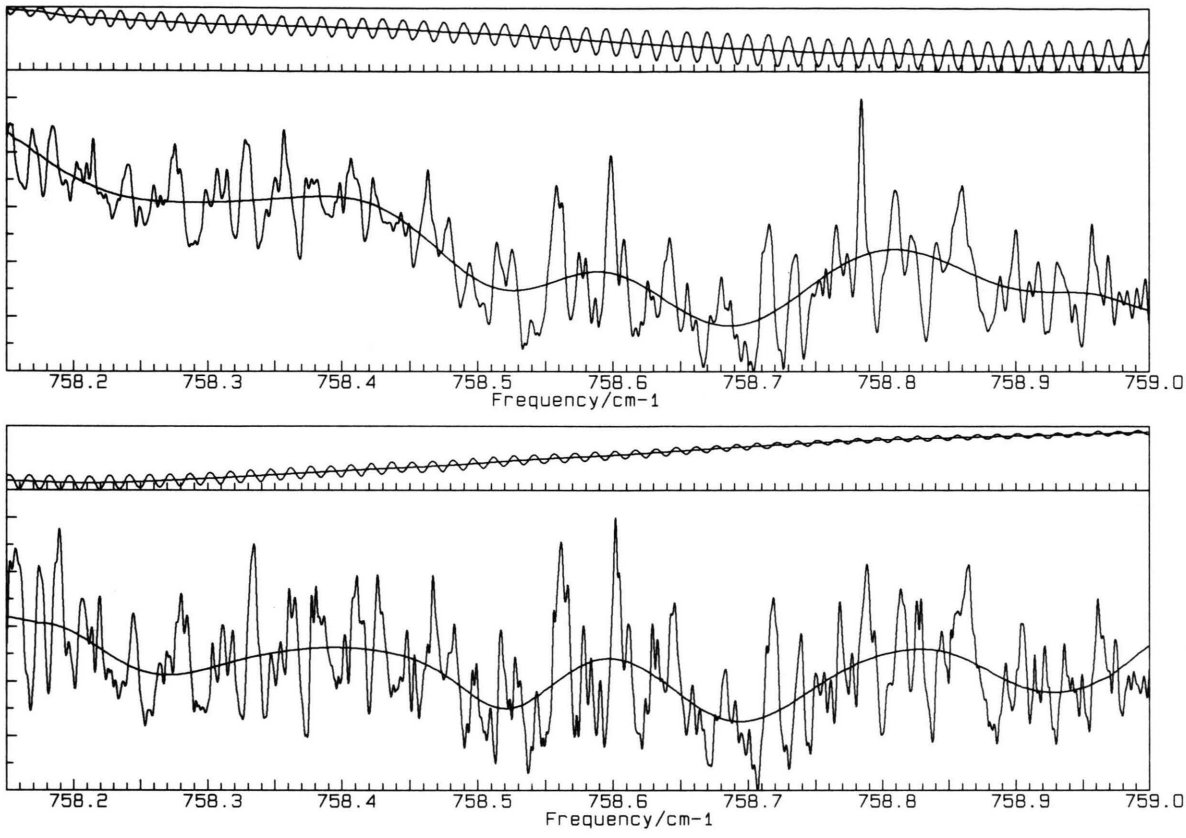

Fig. 3. Spectra as in Fig. 2, amplified numerically relative to the background.

and −75 °C, respectively, are shown in Figure 2. The linear frequency scale was generated as described previously [11] after storing the original absorption and fringe pattern in a microprocessor system. In all cases, calibration was carried out relative to accurately known molecular CO_2, NH_3, and HCN signals [15–18]. Even under the low-pressure, long-path conditions used in obtaining the spectra of Fig. 2, only a week structure appears on top of a strong, continuous background. The same behaviour was found in n-butane FTIR spectra obtained at room temperature with a Bruker IFS 120 HR system at 0.002 cm^{-1} resolution, in the CH_2-rocking region. We have plotted rigid-rotor computer simulated spectra of the overlapping in-phase CH_2-rocking modes, using the molecular stuctures of trans and gauche butane given by Heeman and Bartell [4], and have found dense, partly overlapping but normally completely resolved rovibrational absorptions. It is therefore assumed that the strong, quasi-continuous background in these spectra mainly originates from the addition of rotational components of hot bands and combination bands involving the stack of torsional levels caused by the fundamental near 121 cm^{-1} (trans) and 115 cm^{-1} (gauche) measured and assigned by Stidham and Durig [6] and Compton et al. [5].

In Fig. 3, the intensity modulations in the upper and lower part of Fig. 2 were enhanced relative to the continuous background near 90% and 75% absorption, respectively. The curved horizontal lines like in Fig. 2, extend parallel to the low-frequency Fourier contributions of the signal and serve as intensity thresholds for activating the peak finding routine used to localize the line maximum [11]. The intensity distributions in Fig. 3 resemble much more the expected dense spectra of the CH_2 rocking fundamentals than those in Figure 2. A more quantitative consideration of the signal widths and comparison with the Doppler contribution, which is of the order of 30 MHz, show indeed that single rovibrational transitions are likely to appear among clusters of overlapped structures. It will be shown in the next section that fine structures as

typically seen in Fig. 3 are caused by single rovibrational transitions of the CH_2-rocking fundamental of the trans and gauche n-butane rotamers, and can partly be assigned to semirigid rotor quantum states.

3. Assignments in the 733 cm^{-1} trans CH_2-rocking Fundamental

Trans butane, a $\varkappa = 0.92$ nearly prolate rotor, belongs to the point group C_{2h}. Its infrared-active, in-phase CH_2-rocking fundamental, centered around 733 cm^{-1}, shows A_u symmetry [19] and obeys therefore *c*-type selection rules. From a recent observation of the tunnelling fine structures of rotational transitions of the gauche-butane molecule [12] one can expect that such splittings will be unobservable in Doppler limited vibrational spectra not involving methyl or dihedral torsional levels in both rotamers.

Some gross features of a prolate-rotor spectrum, relative to its band center, can be understood on grounds of the first three terms of the Wang series energy expression [20],

$$E(J, K_a) = \frac{B+C}{2} J(J+1) + \left(A - \frac{B+C}{2}\right) K_a^2 - \tfrac{1}{4}(B-C)\, J(J+1)\, \delta_{1K_a}(-1)^{J-K_c} + \ldots, \quad (1)$$

in connection with the absorption-intensity rules discussed by Allen and Cross [21]. Here and in the following, standard notation is used. The validity of this formula successively deteriorates with increasing J and decreasing K_a because of the increasing oblate character of the rigid-rotor functions.

For not too small K_a values, (1) predicts a series of $Q_{K_a}(J)$ branches ($\Delta J = 0$, $\Delta K_a = \pm 1$) with pronounced band heads if the sets of upper- and lower-state rotational constants, A', B', C' and A'', B'', C'' do not differ appreciably. Such band heads, regularly spaced by $2A' - B' - C' = (1.42 \pm 0.05)$ cm^{-1}, could easily be seen in a 0.05 cm^{-1}-resolution Nicholet FTIR recording. The K_a assignments of the Q branches were thus immediately obvious.

Assignment of individual J components were possible in the strong series $^{R}R_J(J)$ and $^{P}P_J(J)$, each consisting of unresolved doublets $K_c = 0$ and $K_c = 1$. Equation (1), well suited for analysing these transitions, leads to the frequency expression

$$\nu(J) = \nu_0 \pm \tfrac{1}{2}(B'+C') \pm (2J+1)\, A' \quad (2)$$

if the differences in the upper- and lower state rotational constants are neglected. The upper sign holds for the ^{R}R-, the lower for the ^{P}P-subbranches, and ν_0 means the band center. Equation (2) predicts a series of equidistant lines, which was readily found with a spacing of $2A' = (0.240 \pm 0.001)$ in the high-resolution FTIR spectrum available. Individual frequencies and their assignments are listed in Table 3.

Since ν_0 could be accurately determined in a series of symmetric transitions via (2), it was possible to identify individual J components in the branches $^{R}Q_0$ and $^{P}Q_1$. These are the strongest transitions near the origin. A high-resolution FTIR spectrum is shown in Fig. 4, and individual frequencies, up to $J = 50$, are again collected in Table 3. As can be seen in the figure, a complication arises from a change in sign of the $^{P}Q_1$ frequency progression, which is an example of violation of (1) discussed above.

Higher Q_{K_a} branches have not been analysed, as the close spacing of J components and the occurrence of K doubling or appearance of $\Delta K_a = 0$ and $\Delta K_c = 2$ subbranches [21] makes unequivocal assignments unfeasible. The identified but quantitatively not analysed negative $^{P}Q_9$ progression is shown in the diode laser spectrum of Figure 5. The assignment of the leading transition, $J = 9$, is somewhat uncertain owing to background variations. From (1), the spacing between components J and $J+1$ in a band head is

$$\Delta\nu^{Q} = (B' + C' - B'' - C'')(J+1). \quad (3)$$

Thus, the $^{P}Q_9$ sequence shows that $B+C$ is larger in the ground than in the excited state by a small amount.

Some members of higher $^{P}P_{K_a}(J)$ branches are also indicated in Figure 5. Their assignment, and also the

Table 2. Least-squares spectral parameters of the 733 cm^{-1} band of trans butane obtained with the 300 transitions listed in Table 3. Errors given in parentheses in units of the least significant figure are standard deviations. I^r representation and Watson's A reduction were used [23]. The standard deviation of the fit was $\sigma = 0.0018$ cm^{-1}.

	Ground state parameters	Upper state parameters
ν_0/cm^{-1}		733.5797 (5)
A/MHz	22 973.4 (23)	22 974.3 (25)
B/MHz	3 627.0 (10)	3 623.7 (11)
C/MHz	3 409.2 (13)	3 401.9 (13)
Δ_J/kHz	19.7 (3)	19.4 (3)
Δ_{JK}/kHz	−282.5 (56)	−295.7 (65)
Δ_K/kHz	672.8 (229)	620.8 (297)

Table 3. Assignment of observed rovibrational transitions of the trans-butane conformer and comparison with calculated values as obtained with the spectroscopic parameters in Table 2. (J' K'_a K'_c) are the upper-state, and (J'' K''_a K''_c) the ground-state quantum numbers; frequencies in cm^{-1}.

J'	Ka'	Kc'	J"	Ka"	Kc"	OBSERVED	OBS-CALC	J'	Ka'	Kc'	J"	Ka"	Kc"	OBSERVED	OBS-CALC
19	12	7	20	13	7	712.7180	0.0028	22	7	15	23	8	15	718.3480	0.0005
18	12	6	19	13	6	712.9670	0.0019	21	7	14	22	8	14	718.5950	-0.0017
17	12	5	18	13	5	713.2150	0.0008	20	7	13	21	8	13	718.8380	-0.0004
16	12	4	17	13	4	713.4640	-0.0002	19	7	12	20	8	12	719.0810	0.0008
14	12	2	15	13	2	713.9560	0.0010	18	7	11	19	8	11	719.3240	0.0008
12	12	0	13	13	0	714.4470	0.0013	17	7	10	18	8	10	719.5680	0.0010
16	11	5	17	12	5	714.7190	-0.0018	16	7	9	17	8	9	719.8110	0.0015
14	11	3	15	12	3	715.2120	-0.0029	15	7	8	16	8	8	720.0550	0.0004
13	11	2	14	12	2	715.4560	-0.0008	14	7	7	15	8	7	720.2990	-0.0013
12	11	1	13	12	1	715.7020	-0.0019	13	7	6	14	8	6	720.5430	-0.0025
11	11	0	12	12	0	715.9440	-0.0004	12	7	5	13	8	5	720.7840	-0.0012
46	10	36	47	11	36	708.5630	-0.0017	11	7	4	12	8	4	721.0250	-0.0005
45	10	35	46	11	35	708.8080	-0.0015	10	7	3	11	8	3	721.2670	-0.0014
44	10	34	45	11	34	709.0540	-0.0018	9	7	2	10	8	2	721.5070	-0.0003
43	10	33	44	11	33	709.3000	-0.0013	8	7	1	9	8	1	721.7470	0.0004
42	10	32	43	11	32	709.5480	-0.0033	7	7	0	8	8	0	721.9860	0.0014
41	10	31	42	11	31	709.7940	-0.0018	30	6	24	31	7	24	717.6970	0.0019
40	10	30	41	11	30	710.0390	-0.0006	29	6	23	30	7	23	717.9410	0.0001
39	10	29	40	11	29	710.2870	-0.0008	28	6	22	29	7	22	718.1850	-0.0006
38	10	28	39	11	28	710.5340	-0.0003	27	6	21	28	7	21	718.4270	0.0007
37	10	27	38	11	27	710.7800	0.0014	26	6	20	27	7	20	718.6700	0.0006
36	10	26	37	11	26	711.0270	0.0025	25	6	19	26	7	19	718.9130	0.0010
35	10	25	36	11	25	711.2760	0.0010	24	6	18	25	7	18	719.1560	0.0007
34	10	24	35	11	24	711.5230	0.0021	23	6	17	24	7	17	719.4000	-0.0001
33	10	23	34	11	23	711.7720	0.0014	22	6	16	23	7	16	719.6420	0.0009
32	10	22	33	11	22	712.0200	0.0014	12	6	6	13	7	6	722.0670	0.0018
31	10	21	32	11	21	712.2680	0.0019	11	6	5	12	7	5	722.3090	0.0003
30	10	20	31	11	20	712.5170	0.0015	10	6	4	11	7	4	722.5490	0.0017
29	10	19	30	11	19	712.7650	0.0017	9	6	3	10	7	3	722.7900	0.0004
28	10	18	29	11	18	713.0130	0.0016	7	6	1	8	7	1	723.2690	0.0011
27	10	17	28	11	17	713.2610	0.0018	6	6	0	7	7	0	723.5090	0.0004
26	10	16	27	11	16	713.5090	0.0019	24	5	19	25	6	19	720.4600	0.0000
25	10	15	26	11	15	713.7570	0.0019	23	5	18	24	6	18	720.7010	0.0012
24	10	14	25	11	14	714.0040	0.0023	22	5	17	23	6	17	720.9430	0.0003
23	10	13	24	11	13	714.2510	0.0029	21	5	16	22	6	16	721.1820	0.0031
22	10	12	23	11	12	714.5000	0.0019	20	5	15	21	6	15	721.4250	0.0026
21	10	11	22	11	11	714.7480	0.0011	19	5	14	20	6	14	721.6670	0.0023
20	10	10	21	11	10	714.9950	0.0011	18	5	13	19	6	13	721.9090	0.0016
19	10	9	20	11	9	715.2420	0.0006	17	5	12	18	6	12	722.1520	0.0005
18	10	8	19	11	8	715.4890	0.0000	16	5	11	17	6	11	722.3930	0.0009
17	10	7	18	11	7	715.7350	0.0000	15	5	10	16	6	10	722.6350	0.0006
16	10	6	17	11	6	715.9810	0.0000	14	5	9	15	6	9	722.8760	0.0013
15	10	5	16	11	5	716.2270	-0.0009	13	5	8	14	6	8	723.1170	0.0013
14	10	4	15	11	4	716.4740	-0.0029	12	5	7	13	6	7	723.3590	-0.0005
13	10	3	14	11	3	716.7170	-0.0013	11	5	6	12	6	6	723.5990	0.0001
12	10	2	13	11	2	716.9620	-0.0021	10	5	5	11	6	5	723.8400	-0.0001
11	10	1	12	11	1	717.2060	-0.0030	9	5	4	10	6	4	724.0800	-0.0002
10	10	0	11	11	0	717.4510	-0.0043	8	5	3	9	6	3	724.3180	0.0006
25	9	16	26	10	16	715.0360	0.0019	7	5	2	8	6	2	724.5570	0.0014
24	9	15	25	10	15	715.2820	0.0027	6	5	1	7	6	1	724.7940	0.0024
23	9	14	24	10	14	715.5280	0.0026	45	0	45	45	1	45	733.1270	0.0033
21	9	12	22	10	12	716.0240	-0.0003	44	0	44	44	1	44	733.1470	0.0001
20	9	11	21	10	11	716.2720	-0.0019	43	0	43	43	1	43	733.1640	-0.0001
19	9	10	20	10	10	716.5160	-0.0006	42	0	42	42	1	42	733.1810	-0.0004
18	9	9	19	10	9	716.7600	0.0009	41	0	41	41	1	41	733.1980	-0.0015
17	9	8	18	10	8	717.0060	0.0002	40	0	40	40	1	40	733.2140	-0.0024
16	9	7	17	10	7	717.2510	0.0006	39	0	39	39	1	39	733.2260	0.0000
15	9	6	16	10	6	717.4990	-0.0027	38	0	38	38	1	38	733.2420	-0.0012
14	9	5	15	10	5	717.7410	-0.0005	37	0	37	37	1	37	733.2540	-0.0003
13	9	4	14	10	4	717.9840	-0.0004	36	0	36	36	1	36	733.2680	-0.0012
12	9	3	13	10	3	718.2300	-0.0026	35	0	35	35	1	35	733.2810	-0.0016
11	9	2	12	10	2	718.4730	-0.0025	34	0	34	34	1	34	733.2910	-0.0011
10	9	1	11	10	1	718.7140	-0.0012	33	0	33	33	1	33	733.3020	-0.0015
9	9	0	10	10	0	718.9550	0.0000	32	0	32	32	1	32	733.3110	-0.0016
37	8	29	38	9	29	713.3770	-0.0008	31	0	31	31	1	31	733.3200	-0.0017
36	8	28	37	9	28	713.6240	-0.0026	30	0	30	30	1	30	733.3260	-0.0016
35	8	27	36	9	27	713.8680	-0.0014	29	0	29	29	1	29	733.3310	-0.0003
34	8	26	35	9	26	714.1140	-0.0020	28	0	28	28	1	28	733.3360	-0.0013
33	8	25	34	9	25	714.3570	0.0003	27	0	27	27	1	27	733.3400	-0.0034
32	8	24	33	9	24	714.6030	-0.0009	26	0	26	26	1	26	733.3400	-0.0028
31	8	23	32	9	23	714.8480	0.0003	25	0	25	25	1	25	733.3390	-0.0034
30	8	22	31	9	22	715.0940	0.0000	24	0	24	24	1	24	733.3350	-0.0022
29	8	21	30	9	21	715.3400	-0.0004	23	0	23	23	1	23	733.3300	-0.0027
28	8	20	29	9	20	715.5830	0.0022	22	0	22	22	1	22	733.3200	-0.0003
27	8	19	28	9	19	715.8320	-0.0009	21	0	21	21	1	21	733.3100	-0.0001
26	8	18	27	9	18	716.0780	-0.0011	20	0	20	20	1	20	733.2990	-0.0016
25	8	17	26	9	17	716.3240	-0.0009	19	0	19	19	1	19	733.2830	-0.0003
24	8	16	25	9	16	716.5690	0.0000	18	0	18	18	1	18	733.2660	0.0003
23	8	15	24	9	15	716.8150	-0.0003	17	0	17	17	1	17	733.2460	0.0011
22	8	14	23	9	14	717.0610	-0.0007	16	0	16	16	1	16	733.2250	0.0013
21	8	13	22	9	13	717.3070	-0.0015	15	0	15	15	1	15	733.2010	0.0023
20	8	12	21	9	12	717.5520	-0.0014	15	0	15	16	1	15	728.5450	0.0020
19	8	11	20	9	11	717.7960	-0.0003	14	0	14	14	1	14	733.1770	0.0025
18	8	10	19	9	10	718.0390	0.0010	14	0	14	15	1	14	728.8620	0.0019
17	8	9	18	9	9	718.2840	0.0010	13	0	13	14	1	13	729.1730	0.0007
16	8	8	17	9	8	718.5290	-0.0008	13	0	13	13	1	13	733.1510	0.0035
15	8	7	16	9	7	718.7720	0.0006	12	0	12	12	1	12	733.1270	0.0026
14	8	6	15	9	6	719.0170	-0.0011	12	0	12	13	1	12	729.4770	0.0001
13	8	5	14	9	5	719.2590	0.0001	11	0	11	12	1	11	729.7740	0.0003
12	8	4	13	9	4	719.5020	-0.0002	11	0	11	11	1	11	733.1010	0.0025
11	8	3	12	9	3	719.7450	-0.0004	10	0	10	10	1	10	733.0800	-0.0016
10	8	2	11	9	2	719.9890	-0.0021	13	1	13	13	0	13	733.9170	-0.0013
9	8	1	10	9	1	720.2300	-0.0022	14	1	14	14	0	14	733.8800	-0.0014
8	8	0	9	9	0	720.4730	-0.0040	15	1	15	15	0	15	733.8430	-0.0012
29	7	22	30	8	22	716.6380	-0.0010	16	1	16	16	0	16	733.8060	-0.0004
27	7	20	28	8	20	717.1250	0.0013	17	1	17	17	0	17	733.7700	-0.0001
26	7	19	27	8	19	717.3730	-0.0018	18	1	18	18	0	18	733.7350	0.0005
25	7	18	26	8	18	717.6160	-0.0003	19	1	19	19	0	19	733.7010	0.0002
24	7	17	25	8	17	717.8580	0.0021	20	1	20	20	0	20	733.6700	-0.0004
23	7	16	24	8	16	718.1020	0.0027	21	1	21	21	0	21	733.6380	0.0004

Table 3 (continued)

J'	Ka'	Kc'	J"	Ka"	Kc"	OBSERVED	OBS-CALC	J'	Ka'	Kc'	J"	Ka"	Kc"	OBSERVED	OBS-CALC
22	1	22	22	0	22	733.6090	-0.0002	18	6	12	17	5	12	744.9020	0.0009
23	1	23	23	0	23	733.5810	-0.0003	19	6	13	18	5	13	745.1320	0.0014
24	1	24	24	0	24	733.5550	-0.0002	20	6	14	19	5	14	745.3590	0.0031
25	1	25	25	0	25	733.5290	-0.0004	21	6	15	20	5	15	745.5890	0.0030
26	1	26	26	0	26	733.5060	-0.0008	22	6	16	21	5	16	745.8180	0.0025
27	1	27	27	0	27	733.4830	-0.0013	7	7	0	6	6	0	743.6470	-0.0034
28	1	28	28	0	28	733.4610	-0.0014	8	7	1	7	6	1	743.8810	-0.0035
29	1	29	29	0	29	733.4400	-0.0014	10	7	3	9	6	3	744.3480	-0.0018
30	1	30	30	0	30	733.4200	-0.0021	11	7	4	10	6	4	744.5810	-0.0013
31	1	31	31	0	31	733.4000	-0.0022	12	7	5	11	6	5	744.8170	-0.0033
32	1	32	32	0	32	733.3800	-0.0025	13	7	6	12	6	6	745.0500	-0.0034
33	1	33	33	0	33	733.3610	-0.0026	14	7	7	13	6	7	745.2820	-0.0029
34	1	34	34	0	34	733.3420	-0.0021	16	7	9	15	6	9	745.7450	0.0000
35	1	35	35	0	35	733.3240	-0.0024	17	7	10	16	6	10	745.9770	-0.0003
36	1	36	36	0	36	733.3060	-0.0028	18	7	11	17	6	11	746.2070	0.0020
37	1	37	37	0	37	733.2880	-0.0028	19	7	12	18	6	12	746.4370	0.0030
38	1	38	38	0	38	733.2680	-0.0018	20	7	13	19	6	13	746.6680	0.0029
39	1	39	39	0	39	733.2500	-0.0018	21	7	14	20	6	14	746.8990	0.0028
40	1	40	40	0	40	733.2310	-0.0006	22	7	15	21	6	15	747.1300	0.0015
41	1	41	41	0	41	733.2120	0.0002	25	7	18	24	6	18	747.8180	0.0021
42	1	42	42	0	42	733.1930	0.0006	26	7	19	25	6	19	748.0450	0.0033
43	1	43	43	0	43	733.1740	0.0017	27	7	20	26	6	20	748.2730	0.0029
44	1	44	44	0	44	733.1540	0.0030	28	7	21	27	6	21	748.5030	0.0007
45	1	45	45	0	45	733.1360	0.0027	29	7	22	28	6	22	748.7280	0.0023
46	1	46	46	0	46	733.1170	0.0021	30	7	23	29	6	23	748.9550	0.0015
47	1	47	47	0	47	733.0970	0.0038	31	7	24	30	6	24	749.1810	0.0010
48	1	48	48	0	48	733.0800	0.0016	32	7	25	31	6	25	749.4060	0.0009
49	1	49	49	0	49	733.0600	0.0030	33	7	26	32	6	26	749.6300	0.0015
50	1	50	50	0	50	733.0390	0.0038	34	7	27	33	6	27	749.8540	0.0013
8	5	3	7	4	3	741.2860	-0.0018	35	7	28	34	6	28	750.0780	0.0007
9	5	4	8	4	4	741.5170	0.0001	36	7	29	35	6	29	750.3010	0.0006
10	5	5	9	4	5	741.7490	0.0005	37	7	30	36	6	30	750.5230	0.0004
11	5	6	10	4	6	741.9800	0.0012	38	7	31	37	6	31	750.7440	0.0001
12	5	7	11	4	7	742.2130	0.0006	39	7	32	38	6	32	750.9650	-0.0007
13	5	8	12	4	8	742.4440	0.0007	40	7	33	39	6	33	751.1850	-0.0012
14	5	9	13	4	9	742.6770	-0.0005	41	7	34	40	6	34	751.4050	-0.0027
15	5	10	14	4	10	742.9070	0.0000	42	7	35	41	6	35	751.6230	-0.0029
16	5	11	15	4	11	743.1370	0.0000	43	7	36	42	6	36	751.8400	-0.0024
17	5	12	16	4	12	743.3650	0.0010	44	7	37	43	6	37	752.0550	-0.0015
18	5	13	17	4	13	743.5910	0.0037	45	7	38	44	6	38	752.2710	-0.0024
19	5	14	18	4	14	743.8200	0.0038	8	8	0	7	7	0	745.1750	-0.0027
20	5	15	19	4	15	744.0480	0.0027	9	8	1	8	7	1	745.4100	-0.0026
8	6	2	7	5	2	742.5830	-0.0013	10	8	2	9	7	2	745.6420	-0.0006
9	6	3	8	5	3	742.8190	-0.0041	11	8	3	10	7	3	745.8760	0.0000
10	6	4	9	5	4	743.0510	-0.0027	12	8	4	11	7	4	746.1130	-0.0018
13	6	7	12	5	7	743.7460	0.0007	13	8	5	12	7	5	746.3470	-0.0024
14	6	8	13	5	8	743.9780	0.0009	14	8	6	13	7	6	746.5790	-0.0003
15	6	9	14	5	9	744.2100	0.0002	15	8	7	14	7	7	746.8110	0.0014
16	6	10	15	5	10	744.4410	0.0009	16	8	8	15	7	8	747.0450	0.0015
17	6	11	16	5	11	744.6710	0.0015	17	8	9	16	7	9	747.2770	0.0021

analysis of the $^{R}Q_0$ and $^{P}Q_1$ branches in Fig. 4 were accomplished by simulation and fitting, allowing for the rotor asymmetry, the vibrational-state dependence of the spectroscopic parameters, and fourth-order centrifugal perturbations. The least-squares computations on altogether 300 observed lines were carried out using the program package CDA 4/6 developed by Typke [22]. The I^r representation and Watson's A reduction were used in these calculations [23]. The resulting parameters have been collected in Table 2. The residuals are also given in Table 3 and show satisfactory agreement between theory and experiment.

4. Assignments in the 748 cm^{-1} gauche CH_2-rocking Fundamental

Gauche butane belongs to the point group C_2. Its symmetric CH_2-rocking fundamental, centered around 748 cm^{-1}, shows B symmetry [19] and therefore also c-type selection rules. The asymmetry parameter, $\varkappa = -0.847$ [12], is relatively low in magnitude, and (1) has, therefore, less predictive character here. It follows that a typical Q branch structure, like in the case of trans butane, cannot be recognized in the medium resolved Nicholet spectrum which, however, is caused in part also by the interference of trans absorptions.

Attempts to identify single rovibrational transitions in the dense high-resolution spectrum were aided by the recently determined spectroscopic ground-state parameters which allow the prediction of the gauche-butane vibrational-ground-state levels with microwave accuracy [12]. Some ^{P}P and ^{R}R branches could be identified using these parameters, and the assignments could be verified by the method of combination of differences [21, 11]. It was generally helpful to compare low-temperature diode laser with room temperature high-resolution (FTIR or diode laser) spectra and thus to identify gauche transitions in overlapped re-

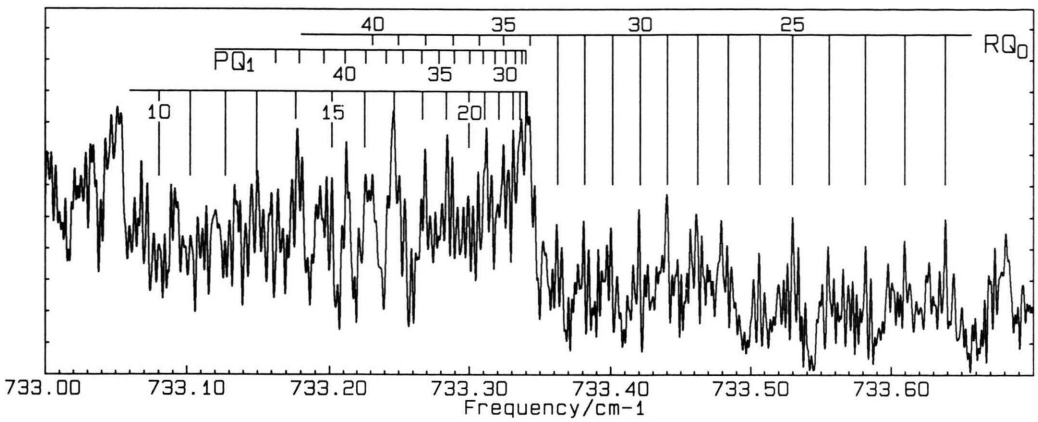

Fig. 4. High-resolution FTIR spectrum of n-butane gas at room temperature showing individual J components of the $K_a=0$, $\Delta K_a=1$ and $K_a=1$, $\Delta K_a=-1$ Q branches of the trans rotamer. The progression of the latter changes sign near $J=25$. The band center is at 733.58 cm^{-1}.

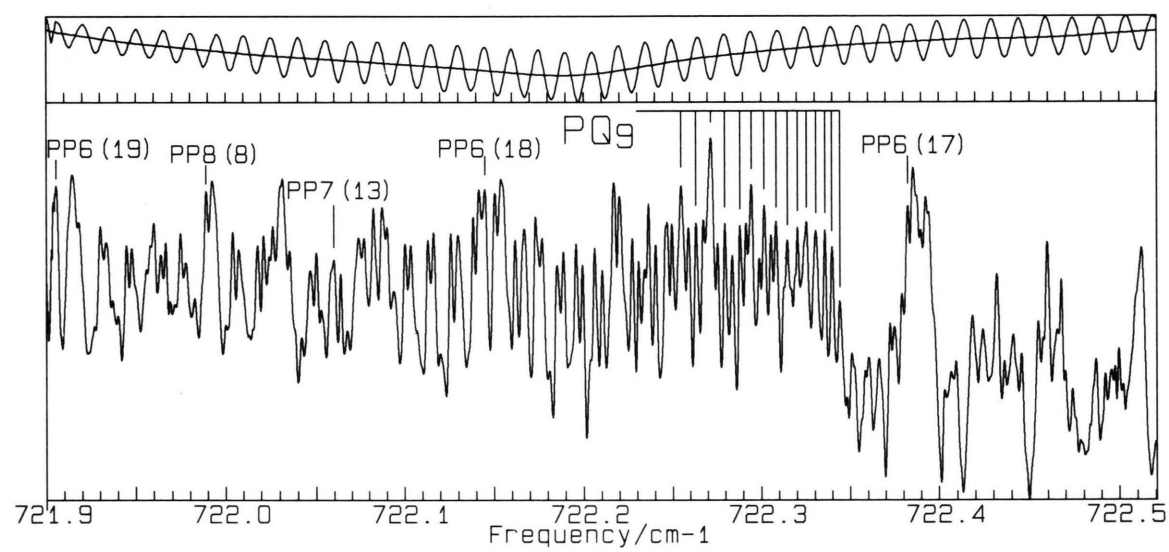

Fig. 5. TDL spectrum of n-butane at 25 °C showing the $^{P}Q_9$ band-head progression and some assigned $^{P}P_{K_a}(J)$ transitions of the trans rotamer. The position of the $J=9$ component of the indicated Q branch is not certain.

gions. Some members of ^{P}P sub-branches assigned in this way are shown in Figure 6. The quantity $B'+C'-B''-C''$ which roughly determines the line separation in Q branches according to (3) is three times larger than in the trans rotamer. It was, therefore, also possible to identify sequences of well separated J members of some Q branches involving projection quantum numbers up to $K_a=4$.

The detailed assignments can be seen in Table 5, and the resulting least-squares spectroscopic parameters have been listed in Table 4.

5. Determination of ΔH

The gauche-trans energy difference was determined from the relative intensities of near-by rovibrational transitions, which depend on the Boltzmann population factors of the ground state involved. Considering a transition $|n\rangle \leftarrow |m\rangle$ in a small frequency range near the center ν_{nm}, its absorption coefficient can be written [21]

$$\alpha_{nm}(\nu) = f_m \frac{N}{c}(1-e^{-\nu_{nm}/kT})\,\nu_{nm}\,B_{nm}\,S(\nu_{nm},\nu), \qquad (4)$$

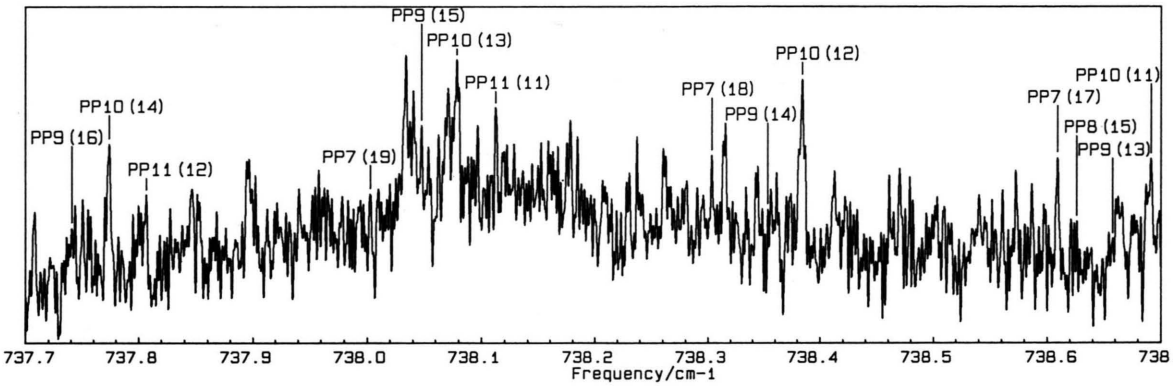

Fig. 6. High-resolution FTIR spectrum of n-butane gas at room temperature. Several $^{P}P_{K_a}(J)$ transitions of the gauche rotamer are indicated.

Table 4. Least-squares spectral parameters of the 748 cm^{-1} band of gauche butane obtained with the 202 transitions listed in Table 5. Errors in parentheses in units of the least significant figure are standard deviations. The ground state rotational and c.d. constants from [12] were held fixed, and the sextic c.d. constants of the upper were constrainted to those of the lower state. I^r representation and Watson's A reduction were used [23]. The standard deviation of the fit was $\sigma = 0.0013$ cm^{-1}.

	Ground state parameters	Upper state parameters
ν_0/cm^{-1}		747.5116 (6)
A/MHz	13 211.92105 (129)	13 212.69 (47)
B/MHz	4 761.72373 (25)	4 761.52 (16)
C/MHz	4 059.68936 (26)	4 031.78 (17)
Δ_J/kHz	4.67201 (28)	5.06 (19)
Δ_{JK}/kHz	−20.2086 (25)	−21.2 (12)
Δ_K/kHz	62.475 (42)	68.4 (42)
δ_J/kHz	1.46428 (10)	1.62 (18)
δ_K/kHz	12.0467 (34)	14.3 (53)
Φ_{JK}/Hz	0.0191 (27)	0.0191
Φ_{KJ}/Hz	−0.782 (63)	−0.782
Φ_K/Hz	3.14 (57)	3.14
φ_J/Hz	0.00315 (10)	0.00315
φ_{JK}/Hz	−0.0927 (34)	−0.0927

where B_{nm}, Einstein's coefficient of induced absorption, is meant to contain the contributions of all degenerate orientational sublevels M_J' and M_J'' in the appropriate radiative polarization state. N is the number density of molecules, c the vacuum speed of light, kT the thermal energy, and S the (Doppler) lineprofile function.

$$f_m = Z^{-1}\, g_m\, e^{-E_m/kT} \tag{5}$$

is the fraction of molecules in the ground state of energy E_m, with Z the partition function of the trans-gauche butane system and g_m the weight factor taking into account nuclear-spin statistics and the geometric weights 2 for the gauche-, and 1 for the trans population. It turns out, however, that an accurate kowledge of g_m is not mandatory for determining the gauche-trans energy difference.

Choosing two neighbouring transitions trans (t) and gauche (g) in their absorption maxima, we can neglect the frequency dependence in (4), yielding

$$\frac{\alpha_{n_t m_t}}{\alpha_{n_g m_g}} = \frac{f_{m_t}}{f_{m_g}} \frac{B_{n_t m_t}}{B_{n_g m_g}}. \tag{6}$$

Introducing

$$\Delta E_{gt} = E_{m_g} - \Delta H - E_{m_t} \tag{7}$$

for the difference of the rotational energy contributions (relative to a common level $J=0$) of gauche and trans molecules in the ground-state, we obtain

$$\ln\left[\frac{\alpha_{n_t m_t}}{\alpha_{n_g m_g}}\right] = \frac{\Delta H + \Delta E_{gt}}{kT} + \ln\left[\frac{g_{m_t}}{g_{m_g}} \frac{B_{n_t m_t}}{B_{n_g m_g}}\right]. \tag{8}$$

Clearly, the last term in (8) does not depend on temperature. The left side is accessible experimentally via Beer's law

$$\alpha_{n_j m_j} = -\frac{1}{x} \ln \frac{I_{n_j m_j}}{I_0}, \quad j = \mathrm{g}, \mathrm{t}, \tag{9}$$

where $I_{n_j m_j}/I_0$ is the fractional absorbed intensity. x, the absorption path length, cancels in comparing transitions. Thus, $\Delta H + \Delta E_{tg}$ can be determined from the temperature variations in (9) and (8), and in turn ΔH could be obtained if ΔE_{tg} were known.

For any pair of trans and gauche transitions, ΔE_{tg} could be calculated if the quantum-state assignments

Table 5. Assignment of experimental rovibrational transitions of the gauche-butane conformer and comparison with calculated values as obtained with the spectroscopic parameters in Table 4, designations as in Table 3.

J'	Ka'	Kc'	J"	Ka"	Kc"	OBSERVED	OBS-CALC	J'	Ka'	Kc'	J"	Ka"	Kc"	OBSERVED	OBS-CALC
11	11	0	12	12	0	737.2341	-0.0010	14	1	14	14	0	14	747.3466	0.0000
11	10	1	12	11	1	737.8067	0.0015	15	1	15	15	0	15	747.3184	0.0002
10	10	0	11	11	0	738.1121	0.0008	16	1	16	16	0	16	747.2901	-0.0008
25	9	16	26	10	16	734.0648	-0.0001	17	1	17	17	0	17	747.2581	0.0005
24	9	15	25	10	15	734.3752	-0.0007	18	1	18	18	0	18	747.2271	-0.0007
23	9	14	24	10	14	734.6850	-0.0006	19	1	19	19	0	19	747.1921	0.0003
22	9	13	23	10	13	734.9929	0.0015	20	1	20	20	0	20	747.1556	0.0011
21	9	12	22	10	12	735.3026	0.0017	21	1	21	21	0	21	747.1189	0.0002
20	9	11	21	10	11	735.6134	0.0008	22	1	22	22	0	22	747.0804	-0.0006
18	9	9	19	10	9	736.2341	-0.0009	6	2	5	6	1	5	748.1402	0.0006
17	9	8	18	10	8	736.5414	0.0008	7	2	6	7	1	6	748.0623	0.0001
16	9	7	17	10	7	736.8504	0.0003	8	2	7	8	1	7	747.9770	0.0007
15	9	6	16	10	6	737.1582	0.0005	9	2	8	9	1	8	747.8902	-0.0008
14	9	5	15	10	5	737.4671	-0.0009	10	2	9	10	1	9	747.8002	0.0007
13	9	4	14	10	4	737.7740	-0.0010	11	2	10	11	1	10	747.7163	-0.0007
12	9	3	13	10	3	738.0786	0.0005	12	2	11	12	1	11	747.6378	-0.0014
11	9	2	12	10	2	738.3844	0.0002	13	2	12	13	1	12	747.5664	-0.0013
10	9	1	11	10	1	738.6900	-0.0008	14	2	13	14	1	13	747.5032	-0.0009
9	9	0	10	10	0	738.9942	-0.0011	15	2	14	15	1	14	747.4475	-0.0001
20	8	12	21	9	12	736.2009	-0.0010	16	2	15	16	1	15	747.3996	-0.0006
19	8	11	20	9	11	736.5053	0.0025	17	2	16	17	1	16	747.3544	0.0010
18	8	10	19	9	10	736.8158	-0.0001	12	3	10	12	2	10	748.3650	-0.0028
17	8	9	18	9	9	737.1240	-0.0005	13	3	11	13	2	11	748.2379	-0.0029
16	8	8	17	9	8	737.4329	-0.0018	14	3	12	14	2	12	748.1065	-0.0017
15	8	7	16	9	7	737.7407	-0.0024	15	3	13	15	2	13	747.9770	-0.0018
14	8	6	15	9	6	738.0476	-0.0025	16	3	14	16	2	14	747.8495	0.0005
13	8	5	14	9	5	738.3535	-0.0020	17	3	15	17	2	15	747.7335	-0.0007
12	8	4	13	9	4	738.6578	-0.0006	18	3	16	18	2	16	747.6263	-0.0001
11	8	3	12	9	3	738.9640	-0.0016	19	3	17	19	2	17	747.5303	0.0011
10	8	2	11	9	2	739.2672	-0.0004	20	3	18	20	2	18	747.4475	0.0009
9	8	1	10	9	1	739.5713	-0.0008	21	3	19	21	2	19	747.3750	0.0009
8	8	0	9	9	0	739.8747	-0.0013	22	3	20	22	2	20	747.3118	0.0004
20	7	13	21	8	13	736.7946	-0.0015	23	3	21	23	2	21	747.2544	0.0006
19	7	12	20	8	12	737.0989	-0.0011	12	4	9	11	3	9	753.0619	0.0035
18	7	11	19	8	11	737.4042	-0.0010	13	4	9	12	3	9	753.1950	0.0003
17	7	10	18	8	10	737.7079	0.0010	13	4	10	12	3	10	753.3655	0.0000
14	7	7	15	8	7	738.6261	0.0003	14	4	10	13	3	10	753.4301	-0.0003
13	7	6	14	8	6	738.9320	-0.0001	14	4	11	14	3	11	749.1040	0.0005
12	7	5	13	8	5	739.2377	-0.0006	15	4	12	15	3	12	748.9734	0.0014
11	7	4	12	8	4	739.5430	-0.0013	16	4	13	16	3	13	748.8282	0.0019
10	7	3	11	8	3	739.8460	-0.0002	17	4	14	17	3	14	748.6734	0.0002
9	7	2	10	8	2	740.1505	-0.0012	18	4	15	18	3	15	748.5074	0.0016
8	7	1	9	8	1	740.4520	0.0000	19	4	16	19	3	16	748.3378	0.0024
7	7	0	8	8	0	740.7544	-0.0004	20	4	17	20	3	17	748.1694	0.0020
18	6	12	19	7	12	738.0027	-0.0015	21	4	18	21	3	18	748.0055	0.0016
17	6	11	18	7	11	738.3033	-0.0011	22	4	19	22	3	19	747.8495	0.0017
16	6	10	17	7	10	738.6080	-0.0034	23	4	20	23	3	20	747.7078	-0.0005
15	6	9	16	7	9	738.9098	-0.0020	24	4	21	24	3	21	747.5787	-0.0012
14	6	8	15	7	8	739.2133	-0.0018	25	4	22	25	3	22	747.4641	-0.0014
13	6	7	14	7	7	739.5171	-0.0017	26	4	23	26	3	23	747.3632	-0.0011
12	6	6	13	7	6	739.8190	0.0003	27	4	24	27	3	24	747.2754	-0.0013
11	6	5	12	7	5	740.1238	-0.0007	7	5	2	6	4	2	752.2018	-0.0012
10	6	4	11	7	4	740.4276	-0.0010	8	5	3	7	4	3	752.4887	-0.0011
9	6	3	10	7	3	740.7287	0.0009	9	5	4	8	4	4	752.7737	-0.0005
8	6	2	9	7	2	741.0299	0.0021	10	5	5	9	4	5	753.0556	0.0014
24	5	20	24	6	18	744.0674	0.0021	11	5	6	10	4	6	753.3392	-0.0009
23	5	19	23	6	17	744.1281	0.0004	11	5	7	10	4	7	753.3424	0.0002
22	5	18	22	6	16	744.1667	0.0021	12	5	7	11	4	7	753.6189	-0.0024
21	5	17	21	6	15	744.1945	0.0008	12	5	8	11	4	8	753.6253	0.0001
20	5	16	20	6	14	744.2105	0.0014	6	6	0	5	5	0	752.5018	0.0019
19	5	15	19	6	13	744.2209	0.0010	7	6	1	6	5	1	752.7919	0.0002
16	5	12	17	6	12	739.1999	-0.0018	8	6	2	7	5	2	753.0781	0.0015
16	5	11	17	6	11	739.2133	0.0005	9	6	3	8	5	3	753.3655	0.0006
15	5	11	16	6	11	739.4996	0.0000	10	6	4	9	5	4	753.6492	0.0024
14	5	9	15	6	9	739.8055	0.0002	11	6	5	10	5	5	753.9345	0.0011
14	5	10	15	6	10	739.8016	-0.0003	12	6	6	11	5	6	754.2157	0.0025
13	5	8	14	6	8	740.1044	0.0009	13	6	7	12	5	7	754.4999	-0.0006
12	5	7	13	6	7	740.4047	0.0015	14	6	8	13	5	8	754.7772	0.0013
11	5	6	12	6	6	740.7065	0.0013	15	6	9	14	5	9	755.0544	0.0010
10	5	5	11	6	5	741.0100	-0.0002	16	6	10	15	5	10	755.3290	0.0004
9	5	4	10	6	4	741.3124	-0.0006	17	6	11	16	5	11	755.5978	0.0019
8	5	3	9	6	3	741.6128	0.0008	18	6	12	17	5	12	755.8635	0.0019
7	5	2	8	6	2	741.9146	0.0004	7	7	0	6	6	0	753.3814	0.0027
6	5	1	7	6	1	742.2145	0.0013	8	7	1	7	6	1	753.6696	0.0021
5	5	0	6	6	0	742.5159	-0.0001	9	7	2	8	6	2	753.9599	-0.0016
8	4	4	9	5	4	742.1969	0.0013	10	7	3	9	6	3	754.2445	-0.0005
7	4	3	8	5	3	742.4996	-0.0014	12	7	5	11	6	5	754.8130	-0.0007
6	4	2	7	5	2	742.7984	-0.0001	13	7	6	12	6	6	755.0966	-0.0019
5	4	1	6	5	1	743.0989	-0.0009	14	7	7	13	6	7	755.3774	-0.0015
4	4	0	5	5	0	743.3966	0.0005	15	7	8	14	6	8	755.6572	-0.0016
26	3	23	26	4	23	747.0086	-0.0001	16	7	9	15	6	9	755.9356	-0.0017
25	3	22	25	4	22	746.9822	-0.0008	17	7	10	16	6	10	756.2105	0.0001
24	3	21	24	4	21	746.9351	0.0001	18	7	11	17	6	11	756.4871	-0.0018
23	3	20	23	4	20	746.8695	-0.0008	8	8	0	7	7	0	754.2628	0.0014
22	3	19	22	4	19	746.7830	-0.0009	9	8	1	8	7	1	754.5497	0.0012
21	3	18	21	4	18	746.6780	-0.0008	10	8	2	9	7	2	754.8356	0.0012
20	3	17	20	4	17	746.5578	-0.0004	11	8	3	10	7	3	755.1207	0.0009
19	3	16	19	4	16	746.4281	-0.0009	12	8	4	11	7	4	755.4044	0.0011
18	3	15	18	4	15	746.2919	-0.0006	13	8	5	12	7	5	755.6886	-0.0002
17	3	15	17	4	13	744.8581	0.0015	14	8	6	13	7	6	755.9699	0.0003
17	3	14	17	4	14	746.1553	-0.0005	15	8	7	14	7	7	756.2499	0.0009
16	3	13	16	4	13	746.0236	-0.0013	16	8	8	15	7	8	756.5299	0.0004
16	3	14	16	4	12	745.0203	0.0025	9	9	0	8	8	0	755.1443	-0.0003
15	3	13	15	4	11	745.1475	0.0013	10	9	1	9	8	1	755.4306	-0.0008
14	3	12	14	4	10	745.2439	-0.0008	11	9	2	10	8	2	755.7149	-0.0001
8	1	8	8	0	8	747.5192	0.0020	12	9	3	11	8	3	755.9980	0.0008
9	1	9	9	0	9	747.4867	0.0004	13	9	4	12	8	4	756.2800	0.0019
10	1	10	10	0	10	747.4563	0.0000	14	9	5	13	8	5	756.5642	-0.0002
11	1	11	11	0	11	747.4293	-0.0014	15	9	6	14	8	6	756.8433	0.0017
12	1	12	12	0	12	747.4029	-0.0022	16	9	7	15	8	7	757.1232	0.0018
13	1	13	13	0	13	747.3742	-0.0004	17	9	8	16	8	8	757.4044	-0.0005

and sufficiently accurate spectral parameters were known. This is not the case here as the analysis of the trans and gauche spectra, as described in the two former sections, was limited to small frequency ranges near the band centers. With the parameters in Tables 2 and 4 it was, however, possible to estimate the frequency positions of certain selected trans and gauche transitions with foreseeable accuracy. It was, therefore, also possible to concentrate on the special trans-gauche pairs fulfilling the condition $|\Delta E_{gt}| \ll \Delta H$, in the following way.

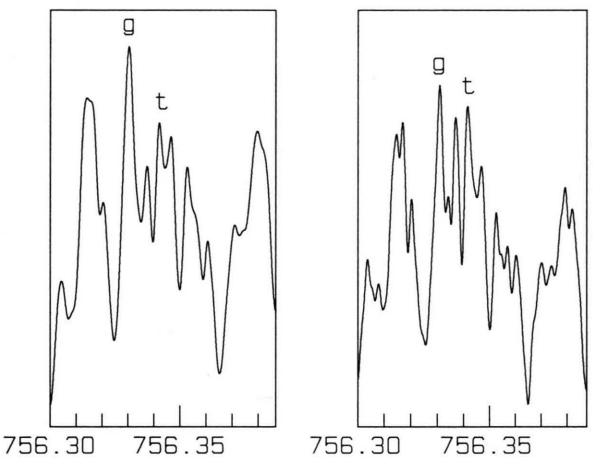

Fig. 7. Selected gauche and trans components in TDL spectra of n-butane gas recorded at temperatures 27 °C (left) and −35 °C (right).

For each assigned trans-gauche pair of this kind, ΔH was calculated from the pair of equations

$$\ln\left[\frac{\ln(I_{n_t m_t}/I_0)}{\ln(I_{n_g m_g}/I_0)}\right]_i = \frac{\Delta H}{kT_i} + \text{const.}, \quad i=1,2, \tag{10}$$

which is easily derived from (8) and (9) under the condition $\Delta E_{gt}=0$. Line shapes were sometimes corrected when perturbed by local background variations or by overlap of near-by absorptions, like in the case of the selected trans and gauche transitions in Figure 7.

Some 40 values ΔH were determined via (10) and their distribution analysed. Many of them could be rejected on physical grounds as not being compatible with the order oif magnitude anticipated from the entries in Table 1. The only significant accumulation of values occurred around 250 cm^{-1} and is considered arising from the increased probability of finding pairs with $\Delta E_{tg} < 20$ cm^{-1} owing to the predictive selection of investigated frequency ranges. There are altogether 14 pairs assigned to this group. The frequency and percentage absorption intensities of the pair members and the temperatures and individual ΔH values have been listed in Table 6. The experimental uncertainties of the latter are estimated to be less than 15%. The final result, obtained as the unweighted statistical

Table 6. Data used to determine ΔH from relative intensities of selected trans and gauche pairs in the CH_2-rocking fundamentals of n-butane, see text. Transition frequencies of the pair members are given in the first and third columns [a], intensities in per cent absorption [b] in the second and fourth columns measured at room temperature [c] and in the sixth and seventh columns at the low temperatures indicated in the second-last column. ΔH values for the individual pairs as obtained with eq. (10) are listed in the last column. The statistical mean is $\Delta H = 246(6)$ cm^{-1} (2.94(7) kJ mol^{-1}, 0.703(17) kcal mol^{-1}).

trans		gauche		T/K	trans	gauche	T/K	ΔH/cm^{-1}
ν/cm^{-1}	Int.	ν/cm^{-1}	Int.		Int.	Int.		
758.1373	22.9	758.1730	21.3	300.0	56.9	35.2	200.0	243
758.4666	23.3	758.4535	17.1	300.0	49.9	23.3	200.0	256
758.2427	10.2	758.3181	15.9	300.0	29.4	26.8	200.0	245
758.5918	10.5	758.5835	20.4	300.0	35.0	38.7	200.0	247
752.1183	16.6	752.1120	16.5	300.0	64.5	34.7	170.0	241
752.1711	11.1	752.1684	14.7	300.0	64.8	43.1	170.0	250
752.1748	12.1	752.1810	14.9	300.0	54.5	32.6	170.0	250
758.2177	25.6	758.2136	24.2	300.0	34.8	20.3	200.0	237
751.4849	15.0	751.4939	14.6	300.0	58.7	33.3	181.0	240
758.1074	20.4	758.0796	15.7	300.0	44.1	21.6	200.0	241
757.5428	15.1	757.5295	11.9	300.0	52.7	26.9	200.0	255
756.1657	16.3	756.1630	19.8	300.0	51.1	47.9	238.0	246
756.3403	15.7	756.3294	24.1	300.0	36.0	41.1	238.0	244
750.0478	15.4	750.0516	22.1	300.0	51.6	55.2	239.0	248

[a] Absolute uncertainty of frequencies is less than 10^{-3} cm^{-1}. – [b] $I/I_0 = 1 - \frac{\text{Int.}}{100}$, see (9). – [c] Variation is (300 ± 2) K.

mean of the entries, is $\Delta H = (246 \pm 18)\ cm^{-1}$. The error means three standard deviations.

It is not feasible to give assignments for the transitions in Table 6 as there are, as already pointed out, several appropriate trans-gauche pairs predicted in a small frequency interval. It should be mentioned that in principle also trans-trans and gauche-gauche pairs may exist showing temperature variations of their relative intensities like the transitions in Table 6. Inspections of line-strength expressions or more simply of computer calculations leave, however, only small probability for finding a strong partner transition originating from a level 250 cm^{-1} above the lower level of the first, belonging to the same rotamer, and falling into the $(755 \pm 5)\ cm^{-1}$ range investigated. In Table 6, only pairs of comparable intensity at room temperature have been taken into account. Similarly, a small probability remains that hot-band transitions might partly be involved in Table 6. This would not affect ΔH within the range of validity of the Born-Oppenheimer approximation, as long as not again a hot-band component was combined with any other transition of the rotamer, which, however, could not be excluded.

6. Conclusion

Diode laser spectra at different probe temperatures and room temperature Fourier transform spectra of n-butane gas have been recorded in the CH_2-rocking region around 740 cm^{-1}. The rovibrational transitions of the trans and gauche rotameric forms appeared, even under low-pressure Doppler limited conditions, weakly on top of a quasicontinuous strong absorption background which is probably caused by the overlap of hot-band transitions carrying one or more quanta of the torsion vibrations around the central C–C bonds in the two stable rotamers. It was possible to firmly identify several series of transitions of the fundamentals which lead to the rovibrational parameters in Table 2 and 4. Extensive assignments were not feasible in the enormously dense spectra. The band centers were accurately determined to be ν_0(trans) $= (733.5797 \pm 0.0015)\ cm^{-1}$ and ν_0(gauche) $= (747.5116 \pm 0.0018)\ cm^{-1}$. The errors are three standard deviations.

The gauche-trans energy difference ΔH was then determined measuring the temperature dependence of the absorption intensities of adjacent strong trans and gauche rovibrational transitions. The trans-gauche pairs were preselected by computer with the aid of the spectral parameters in order to have similar rotational ground-state energies, and identified in the spectra using the criterion of (almost) identical temperature behaviour of relative intensities. The numerical result $\Delta H = (246 \pm 18)\ cm^{-1}$ is included in Table 1 and can be compared with those of previous methods of determination. First of all, it is seen that our value ranges inconsistently lower than that similarly determined from Raman gas-phase spectra in low resolution [2]. Considering uncertainties, there is best agreement with the ab-initio result near 230 cm^{-1}. The trend towards higher values in the gaseous phase as compared with the accurate liquid-phase result of 195 cm^{-1} was found to be present but less pronounced than expected from the previous determinations. Thus, it seems that the liquid-state intermolecular packing forces prospected by Pratt et al. [9] to decrease the gauche-trans energy difference are indeed effective to a measurable extent.

Acknowledgements

The support of the Deutsche Forschungsgemeinschaft and of the Fonds der Chemischen Industrie are gratefully acknowledged. Thanks are due to Professor H. Bürger, Wuppertal, for supporting FTIR butane spectra in medium resolution. The high-resolution FTIR spectra have been recorded with the Bruker IFS 120 HR instrument at the University of Giessen under the supervision of Professor M. Winnewisser and with the technical assistance of Mr. K. Lattner.

[1] G. J. Szasz, M. Sheppard, and D. H. Rank, J. Chem. Phys. **16,** 704 (1948).
[2] A. L. Verma, W. F. Murphy, and H. J. Bernstein, J. Chem. Phys. **60,** 1540 (1974).
[3] S. S. Chen, R. C. Wilholt, and B. J. Zwolinski, J. Phys. Chem. Ref. Data **4,** 859 (1975).
[4] R. K. Heenan and L. S. Bartell, J. Chem. Phys. **78,** 1270 (1983).
[5] D. A. C. Compton, S. Montero, and W. F. Murphy, J. Phys. Chem. **84,** 3587 (1980).
[6] H. D. Stidham and J. R. Durig, Spectrochim. Acta **42 A,** 105 (1986).
[7] K. Raghavachari, J. Chem. Phys. **81,** 1383 (1984).
[8] S. Kint, J. R. Scherer, and R. G. Snyder, J. Chem. Phys. **73,** 2599 (1980).
[9] L. R. Pratt, C. S. Hsu, and D. Chandler, J. Chem. Phys. **68,** 4202 (1978).
[10] W. L. Jorgensen, J. Amer. Chem. Soc. **103,** 4721 (1981).
[11] G. Gassler, B. Reißenauer, and W. Hüttner, Z. Naturforsch. **44 a,** 316 (1989).

[12] W. Hüttner, W. Majer, and H. Kästle, Mol. Phys. **67,** 131 (1989).
[13] G. Tränkle and W. Hüttner, Appl. Opt. **21,** 4151 (1982).
[14] J. U. White, J. Opt. Soc. Amer. **32,** 285 (1942).
[15] R. Paso, J. Kauppinen, and R. Anttila, J. Mol. Spectrosc. **78,** 236 (1980). – K. Jolma, J. Kauppinen, and V.-M. Horneman, J. Mol. Spectrosc. **101,** 300 (1983).
[16] Š. Urban, D. Papoušek, J. Kauppinen, K. Yamada, and G. Winnewisser, J. Mol. Spectrosc. **101,** 1 (1983). – Š. Urban, D. Papoušek, S. P. Belov, A. F. Krupnov, M. Yu Tret'yakov, K. Yamada, and G. Winnewisser, J. Mol. Spectrosc. **101,** 16 (1983).
[17] J. S. Knoll, G. L. Tettemer, W. G. Planet, K. N. Rao, D.-W. Chen, and L. A. Pugh, Appl. Opt. **15,** 2973 (1976). – S. P. Reddy, W. Ivancic, V. M. Devi, A. Baldacci, K. N. Rao, A. W. Mantz, and R. S. Eng, Appl. Opt. **18,** 1350 (1979).
[18] G. Guelachvili and K. N. Rao, Handbook of Infrared Standards, Academic Press Inc., Orlando 1986.
[19] J. K. Brown, N. Sheppard, and D. M. Simpson, Phil. Trans. Roy. Soc. London **A 247,** 35 (1954).
[20] C. H. Townes and A. L. Schawlow, Microwave Spectroscoypy, McGraw-Hill, New York 1955.
[21] H. C., Allen, Jr. and P. C. Cross, Molecular Vib-Rotors, John Wiley, New York 1963.
[22] V. Typke, Spectrochim. Acta **42 A,** I–IV (1986).
[23] J. K. G. Watson, in: Vibrational Spectra and Structure, vol. 6 (J. R. Durig, ed.), Elsevier, Amsterdam 1977.